Geophysical Prospecting

EAGE EUROPEAN ASSOCIATION OF GEOSCIENTISTS & ENGINEERS

Geophysical Prospecting, 2015 doi: 10.1111/1365-2478.12292

Retrieving virtual reflection responses at drill-bit positions using seismic interferometry with drill-bit noise

Yi Liu[1]*, Deyan Draganov[2], Kees Wapenaar[2] and Børge Arntsen[1]

[1]*Department of Petroleum Engineering and Applied Geophysics, Norwegian University of Science and Technology, 7491 Trondheim, Norway, and* [2]*Department of Geoscience and Engineering, Delft University of Technology, 2628 CN Delft, The Netherlands*

Received September 2014, revision accepted February 2015

ABSTRACT

In the field of seismic interferometry, researchers have retrieved surface waves and body waves by cross-correlating recordings of uncorrelated noise sources to extract useful subsurface information. The retrieved wavefields in most applications are between receivers. When the positions of the noise sources are known, inter-source interferometry can be applied to retrieve the wavefields between sources, thus turning sources into virtual receivers. Previous applications of this form of interferometry assume impulsive point sources or transient sources with similar signatures. We investigate the requirements of applying inter-source seismic interferometry using non-transient noise sources with known positions to retrieve reflection responses at those positions and show the results using synthetic drilling noise as source. We show that, if pilot signals (estimates of the drill-bit signals) are not available, it is required that the drill-bit signals are the same and that the phases of the virtual reflections at drill-bit positions can be retrieved by deconvolution interferometry or by cross-coherence interferometry. Further, for this case, classic interferometry by cross-correlation can be used if the source power spectrum can be estimated. If pilot signals are available, virtual reflection responses can be obtained by first using standard seismic-while-drilling processing techniques such as pilot cross-correlation and pilot deconvolution to remove the drill-bit signatures in the data and then applying cross-correlation interferometry. Therefore, provided that pilot signals are reliable, drill-bit data can be redatumed from surface to borehole depths using this inter-source interferometry approach without any velocity information of the medium, and we show that a well-positioned image below the borehole can be obtained using interferometrically redatumed reflection responses with just a simple velocity model. We discuss some of the practical hurdles that restrict the application of the proposed method offshore.

Key words: Borehole geophysics, Imaging, Noise, Seismics.

INTRODUCTION

The cross-correlation of two recordings of seismic noise leads to an estimate of the Green's function between these two positions, as if one of them were an impulsive source. This method has been successfully applied in seismology to retrieve surface waves using coda waves (Campillo and Paul 2003; Snieder 2004) or ambient-noise recordings (Shapiro and Campillo 2004; Sabra *et al.* 2005a), and useful subsurface information has been derived from the retrieved surface waves by seismic tomography (Shapiro *et al.* 2005; Sabra *et al.* 2005b; Yang *et al.* 2007). In general, the method of retrieving the Green's function by cross-correlation is called seismic interferometry (SI). The derivations of such retrieval using diffuse wavefields are shown in Lobkis and Weaver (2001) and Snieder (2004) and for non-diffuse wavefields in any inhomogeneous medium by Wapenaar (2004) and Wapenaar and Fokkema (2006).

Besides surface waves, body waves can also be retrieved by ambient-noise SI, although not that easily mostly because of its stronger amplitude decay with distance. In regional

*E-mail: yi.liu@ntnu.no

seismology, examples of retrieving body waves are shown by Roux *et al.* (2005) and Gerstoft *et al.* (2006) for diving P-waves, by Zhan *et al.* (2010) for Moho-reflected S-waves, and by Ruigrok, Campman, and Wapenaar (2011) for Moho-reflected P-waves.

In exploration seismics, body-wave reflections (above 1 Hz) are usually required for structural imaging. At frequencies above 1 Hz in ambient-noise recordings, the surface waves should be suppressed in order to retrieve the body waves. Night-hour ambient-noise recordings (Draganov *et al.* 2007), patterns of geophones (Draganov *et al.* 2009), and selected parts of the noise (Panea *et al.* 2014) are utilized for such suppression in order to retrieve reflections using ambient noise. Draganov *et al.* (2013) and Xu *et al.* (2012) show examples of extracting exploration-scale velocities and structures from ambient-noise recordings. Cross-coherence is another approach to apply SI using noise sources, and Nakata *et al.* (2011) retrieve both surface waves and body waves from traffic noise by cross-coherence SI.

Besides passive noise, active noise with known locations, such as drill-bit noise, has long been used in seismic-while-drilling (SWD) to obtain reverse vertical seismic profiles (Rector and Marion 1991; Poletto and Miranda 2004) and to provide look-ahead information while drilling (Malusa, Poletto, and Miranda 2002; Eidsvik and Hokstad 2006). Most methods in SWD rely on pilot signals (estimates of the seismic signature of the drill bit) to compress the drill-bit signal to an impulse (Rector and Marion 1991; Poletto, Rocca, and Bertelli 2000; Poletto *et al.* 2004; Poletto *et al.* 2014). Standard SWD processing involves cross-correlation of pilot signals and geophone recordings, reference deconvolution, and pilot-delay shift. An alternative method to process SWD data that do not require pilot signals is shown by Miller, Haldorsen, and Kostov (1990) and Haldorsen, Miller, and Walsh (1995) using multi-channel deconvolution. To apply SI to drill-bit data, Vasconcelos and Snieder (2008b) use deconvolution SI and show both numerical and field examples of using the retrieved reflections for imaging. In their method, pilot signals are not required because the source signature is cancelled by spectral division during deconvolution. Poletto, Corubolo, and Comelli (2010) compared the method of drill-bit SI with and without pilot signals and showed field-data results from cross-correlation and deconvolution SI.

All these applications of SI using noise sources retrieve the estimated Green's function between receivers. Inter-source interferometry is derived by source–receiver reciprocity (Curtis *et al.* 2009) and retrieves the estimated Green's function between sources. This form of SI can be useful for noise sources with known locations. Curtis *et al.* (2009) and Tonegawa and Nishida (2010) show examples of creating virtual seismometers from different types of earthquakes, assuming the source time functions of the earthquakes are similar.

To investigate the application of inter-source interferometry to non-transient noise sources with and without similar signals, we use synthetic drill-bit data from drilling noise in a horizontal well to retrieve virtual reflection responses at drill-bit positions. Practicalities of drill-string multiples and pilot-delay shift are not included. We first look at the basic equations of inter-source interferometry by cross-correlation, deconvolution, and cross-coherence and then show the results from each approach. A migration image below the well using the retrieved reflection responses is compared with a surface–seismic image to show the potential advantage of using inter-source SI with drill-bit data.

EQUATIONS OF SEISMIC INTERFEROMETRY

It is known from seismic interferometry (SI) that new seismic responses between two locations can be retrieved by cross-correlating the observed wavefields at these locations and summing over surrounding sources. The summation is implicit when recordings from ambient noise are used because the recorded wavefield is already a superposition of simultaneously acting noise sources. Supposing that a response from each individual impulsive point source is measured separately, and using acoustic Green's function representations, SI by cross-correlation can be represented in the frequency domain (Wapenaar and Fokkema 2006) as

$$G(\mathbf{x}_A|\mathbf{x}_B) + G^*(\mathbf{x}_A|\mathbf{x}_B) \propto \oint_{\partial D} G^*(\mathbf{x}_A|\mathbf{x}) G(\mathbf{x}_B|\mathbf{x}) d\mathbf{x}. \quad (1)$$

Here, the Green's function $G(\mathbf{x}_A|\mathbf{x}_B)$ represents the acoustic wavefield observed at $\mathbf{x}_A$ due to an impulsive point source at $\mathbf{x}_B$. Using the Cartesian coordinate vector, spatial location is denoted by $\mathbf{x} = (x, y, z)$ with z pointing downward, representing depth. Uppercase symbols represent quantities in the frequency domain. The superscript * denotes complex conjugate. Therefore, in the time domain, the left-hand side of equation (1) represents the superposition of the causal and anti-causal responses observed at $\mathbf{x}_A$ due to an impulsive point source at $\mathbf{x}_B$, and it is proportional to a surface integral of cross-correlations of the Green's functions observed at $\mathbf{x}_A$ and $\mathbf{x}_B$ due to sources at all $\mathbf{x}$ at a boundary ∂D. Equation (1) is a high-frequency approximation; it is further assumed that the

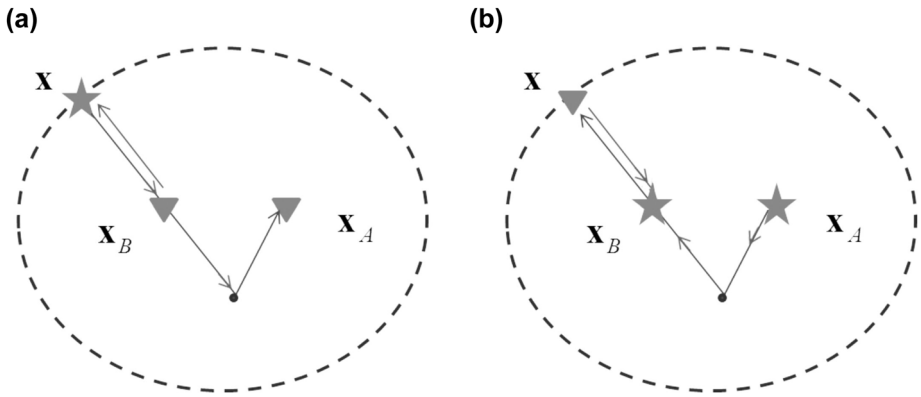

Figure 1 Illustration of SI of a) inter-receiver form and b) inter-source form. Triangle denotes the receiver, and star denotes the source. Dashed line indicates the integral surface. The direct-wave travel path is rotated to show that complex conjugation is taken:

medium at and outside ∂D is homogeneous and that all rays leaving the source boundary are approximately normal to ∂D (Wapenaar and Fokkema 2006).

Inter-source interferometry can be formed by source–receiver reciprocity (Curtis *et al.* 2009). By using $G^*(\mathbf{x}_A|\mathbf{x}) = G^*(\mathbf{x}|\mathbf{x}_A)$ and $G(\mathbf{x}_B|\mathbf{x}) = G(\mathbf{x}|\mathbf{x}_B)$, the right-hand side of equation (1) turns into

$$G(\mathbf{x}_A|\mathbf{x}_B) + G^*(\mathbf{x}_A|\mathbf{x}_B) \propto \oint_{\partial D} G^*(\mathbf{x}|\mathbf{x}_A)G(\mathbf{x}|\mathbf{x}_B)d\mathbf{x}. \quad (2)$$

It can be interpreted from this equation that, instead of the Green's function between two receivers, the cross-correlation of the response at $\mathbf{x}$ due to the impulsive point sources at $\mathbf{x}_A$ and at $\mathbf{x}_B$, as well as the subsequent summation of the correlated responses over all receiver positions, retrieves the estimated Green's function between two sources.

In reality, an impulsive point source is replaced by a source with a time function $s(t)$, which can be either transient or non-transient (e.g., noise). Because, in this paper, we consider drill-bit data, we will assume from here onward that $s(t)$ is a random non-transient signal. We write the observed response at $\mathbf{x}$ due to the source at $\mathbf{x}_i$ (i can be A or B) as

$$Y(\mathbf{x}|\mathbf{x}_i) = G(\mathbf{x}|\mathbf{x}_i)S(\mathbf{x}_i), \quad (3)$$

where $S(\mathbf{x}_i)$ is the source function at $\mathbf{x}_i$ in the frequency domain (i.e., the source spectrum). Further, we define C_{AB} as

$$C_{AB}(\mathbf{x}) = Y^*(\mathbf{x}|\mathbf{x}_A)Y(\mathbf{x}|\mathbf{x}_B). \quad (4)$$

Then, for an acquisition geometry with sources in the subsurface and receivers at the surface ∂D_0, the summation of C_{AB} over all available receiver positions on ∂D_0 reads

$$\int_{\partial D_0} C_{AB}(\mathbf{x})d\mathbf{x} = S^*(\mathbf{x}_A)S(\mathbf{x}_B)\int_{\partial D_0} G^*(\mathbf{x}|\mathbf{x}_A)G(\mathbf{x}|\mathbf{x}_B)d\mathbf{x}. \quad (5)$$

Constructive contribution to the retrieved Green's function comes from stationary-phase positions (Snieder, Wapenaar, and Larner 2006). For retrieving the reflections from below the subsurface sources, the stationary points lie along the surface where we can have our measurements. Spurious events may occur not only due to finite aperture available on the surface ∂D_0 but also due to the one-sided illumination of having receivers only at the surface and also due to intrinsic losses in the medium. Overall, given a wide coverage on the surface ∂D_0 and compared with equation (2), equation (5) becomes

$$\int_{\partial D_0} C_{AB}(\mathbf{x})d\mathbf{x} \propto S^*(\mathbf{x}_A)S(\mathbf{x}_B)(G(\mathbf{x}_A|\mathbf{x}_B) + G^*(\mathbf{x}_A|\mathbf{x}_B)), \quad (6)$$

where $G(\mathbf{x}_A|\mathbf{x}_B)$ mainly contains reflections from one side of the sources because of the one-sided summation along ∂D_0 (reflections from the other side of the sources would result in non-physical arrivals because ∂D_0 is not a closed boundary (Snieder *et al.* 2006). Now we have $S^*(\mathbf{x}_A)S(\mathbf{x}_B)$ on the right-hand side, and when $S(\mathbf{x}_A) \neq S(\mathbf{x}_B)$, $S^*(\mathbf{x}_A)S(\mathbf{x}_B)$ has a random phase and therefore changes the phase of the retrieved Green's function on the right-hand side. This does not happen for inter-receiver SI because the left-hand side of equation (1) is always the cross-correlation of the responses from the same source. This can be understood more intuitively from Fig. 1, where the direct-wave travel path is rotated to show that complex conjugation is taken. In panel a), the recorded wavefields represented by the ray paths with opposite arrows are cross-correlated and the travel time on the common path can be found and subtracted because they are from the same physical source. However, this is not the case for inter-source SI shown in Fig. 1 b) because the ray path with opposite arrows originates from different sources, and when the random source signals are different, cross-correlation does not find the

common travel path, except when $\mathbf{x}_A = \mathbf{x}_B$, i.e., the zero-offset virtual traces[1].

Sources with the same signal

If we consider the special case of both sources with the same signature, e.g., $S(\mathbf{x}_A) = S(\mathbf{x}_B) = S$, equation (6) becomes

$$\int_{\partial D_0} C_{AB}(\mathbf{x})d\mathbf{x} \propto |S|^2(G(\mathbf{x}_A|\mathbf{x}_B) + G^*(\mathbf{x}_A|\mathbf{x}_B)). \tag{7}$$

The right-hand side yields, in the time domain, the Green's function between two sources $\mathbf{x}_A$ and $\mathbf{x}_B$ convolved with the autocorrelation of the source signal. If the autocorrelation does not resemble the Dirac delta function $\delta(t)$, the amplitude information in the Green's function will be distorted, but this problem could be alleviated by deconvolving the power spectrum $|S|^2$ from C_{AB} if such information is available.

If $|S|^2$ is unknown, deconvolution SI (Vasconcelos and Snieder 2008a) or cross-coherence SI (Nakata *et al.* 2011) can be used, and they are defined in the frequency domain as

$$D_{AB}(\mathbf{x}) = \frac{Y(\mathbf{x}|\mathbf{x}_B)}{Y(\mathbf{x}|\mathbf{x}_A)} = \frac{Y^*(\mathbf{x}|\mathbf{x}_A)Y(\mathbf{x}|\mathbf{x}_B)}{|Y(\mathbf{x}|\mathbf{x}_A)|^2} = \frac{G^*(\mathbf{x}|\mathbf{x}_A)G(\mathbf{x}|\mathbf{x}_B)}{|G(\mathbf{x}|\mathbf{x}_A)|^2} \tag{8}$$

and

$$H_{AB}(\mathbf{x}) = \frac{Y^*(\mathbf{x}|\mathbf{x}_A)Y(\mathbf{x}|\mathbf{x}_B)}{|Y(\mathbf{x}|\mathbf{x}_A)||Y(\mathbf{x}|\mathbf{x}_B)|} = \frac{G^*(\mathbf{x}|\mathbf{x}_A)G(\mathbf{x}|\mathbf{x}_B)}{|G(\mathbf{x}|\mathbf{x}_A)||G(\mathbf{x}|\mathbf{x}_B)|}, \tag{9}$$

respectively. The source signature is cancelled by the spectral division in both equations. Although the amplitude information is discarded, the phase information is kept in both approaches, which is acceptable for structural imaging or tomography. Both D_{AB} and H_{AB} are equal to 1 when $\mathbf{x}_A = \mathbf{x}_B$, which results in the Dirac delta function in time at zero offset. This means that the retrieved responses by both approaches satisfy the so-called *clamped boundary condition* (Vasconcelos and Snieder 2008a). It can also be recognized from equation (8) that, for deconvolution SI, the denominator changes when we interchange $\mathbf{x}_A$ and $\mathbf{x}_B$, whereas for cross-coherence SI, the denominator does not change. Therefore, cross-coherence removes the effect from amplitude variations and gives a more balanced result. In addition, cross-coherence is also more numerically stable because, when the denominator is small, the numerator is also small. Nakata *et al.* (2011) provide a detailed analysis of the properties of cross-coherence SI. Next, integrating both sides of equations (8) and (9) along ∂D_0 reads

$$\int_{\partial D_0} D_{AB}(\mathbf{x})d\mathbf{x} = \int_{\partial D_0} \frac{G^*(\mathbf{x}|\mathbf{x}_A)G(\mathbf{x}|\mathbf{x}_B)}{|G(\mathbf{x}|\mathbf{x}_A)|^2}d\mathbf{x} \tag{10}$$

and

$$\int_{\partial D_0} H_{AB}(\mathbf{x})d\mathbf{x} = \int_{\partial D_0} \frac{G^*(\mathbf{x}|\mathbf{x}_A)G(\mathbf{x}|\mathbf{x}_B)}{|G(\mathbf{x}|\mathbf{x}_A)||G(\mathbf{x}|\mathbf{x}_B)|}d\mathbf{x}. \tag{11}$$

Comparing with equation (2), it shows that the phase of the Green's function between sources can be estimated without knowing the individual source signals.

Sources with different signals

For sources with different signals, it is required that the estimates of the source signals are known in order to apply inter-source interferometry. For drill-bit SI, it means applying standard SWD processing (Rector and Hardage 1992; Poletto *et al.* 2004) using pilot signals before applying SI. We briefly describe such drill-bit signal deconvolution as

$$\widetilde{G}(\mathbf{x}|\mathbf{x}_A) = \frac{Y(\mathbf{x}|\mathbf{x}_A)\widetilde{S}^*(\mathbf{x}_A)}{|\widetilde{S}(\mathbf{x}_A)|^2}. \tag{12}$$

Here, $\widetilde{S}(\mathbf{x}_A)$ is the pilot signal of the drill bit at $\mathbf{x}_A$, and $\widetilde{G}(\mathbf{x}|\mathbf{x}_A)$ represents the estimated impulse response from the drill bit to the receiver. Related technique and discussion on drill-bit data processing can be found in Poletto *et al.* (2004). Then one can use the classic cross-correlation approach shown in equation (2) to estimate the Green's function between sources.

As briefly mentioned earlier, the zero-offset virtual traces can still be recovered when the source signals are different and no pilot signal is measured. However, in this zero-offset case, when SI by autocorrelation is to be used, it follows from equation (6) that the right-hand side still contains $|S|^2$. This means that the virtual zero-offset response, even though zero-phased, is still blurred by the autocorrelation of the drill-bit signal. This is equivalent to the inter-receiver-type SI by cross-correlation using noise source signal, which is not necessarily white by itself. In practical applications, this would mean that the correlation of the drill-bit noise will not be a delta function and the zero-offset reflection response would suffer from a virtual-source wavelet with long duration. In contrast, when pilot signals are measured, the approach described by equations (2) and (12) leads to a virtual-source response with a short-duration wavelet.

[1] One of the reviewers pointed us to the patent: Mateeva A., Mehta K. and Tatanova M. 2011. Look Ahead Seismic While Drilling, international publication No. WO 2011/159803 A2, in which a zero-offset version of the method is presented.

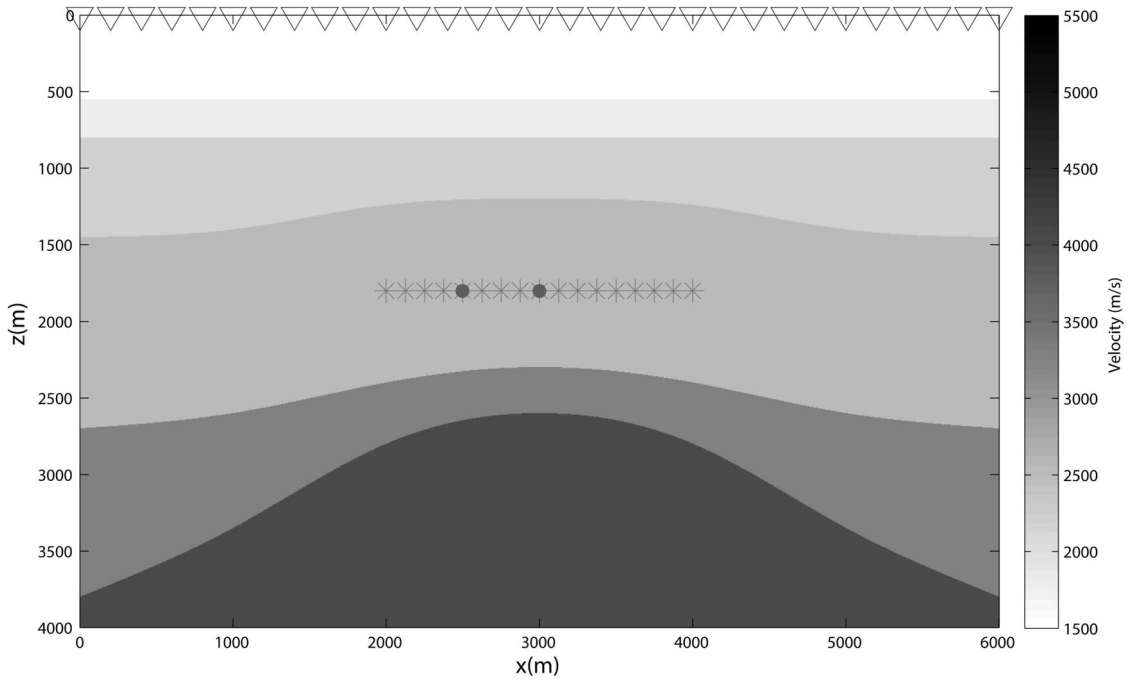

Figure 2 The P-wave velocity model. Triangle denotes the receiver, and star denotes the drill-bit source position. The two solid circles indicate the reference positions. Every fifth source and receiver are plotted.

NUMERICAL DRILL-BIT EXAMPLES

Based on the analysis from the previous section, we assume two situations: one in which we use the drill bit with the same signal (just for illustration) and one with different signals in acoustic medium. The 2D P-wave velocity model is shown in Fig. 2. We place 121 receivers (denoted by triangles) at the surface with a spacing of 50 m. The first receiver is at $x = 0$ m, and the last receiver is at $x = 6000$ m. The drill bit is in a horizontal well at the depth $z = 1800$ m, and we model 81 common-source gathers at the drill-bit positions (denoted by stars) from $x = 2000$ m to $x = 4000$ m with a spacing of 25 m.

Same source signal

Although in practice a drill bit emits signals that are different from each other, we include this special case of them having the same signal for any general non-transient noise and to demonstrate that deconvolution or cross-coherence interferometry can be used to retrieve inter-source reflections in this case. These two approaches do not rely on the assumption that the autocorrelation of noise signal is spike-like.

The modelled drill-bit source function and its power spectrum are shown in Fig. 3 c) and d), respectively. The modelled drilling noise is 3 seconds long, and we convolve the drill-bit signal with the sources modelled using a Ricker wavelet by an acoustic finite-difference method (Thorbecke and Draganov 2011). Fig. 3 a) and b) shows the acoustic responses received at the surface from the drill-bit position at $x = 2500$ m and $x = 3000$ m (denoted by two solid circles in Fig. 2), respectively. Because the power spectrum of the drill-bit source function is not white, cross-correlation interferometry is not that suitable without knowing the source power spectrum itself. Thus, assuming no information about the source signal is available, we use deconvolution (equation (8)) and cross-coherence (equation (9)) and sum the results over all receiver positions (eqautions (10) and (11)). Then we apply a low-pass filter up to 40 Hz and assign a Ricker wavelet to the results. Fig. 4 a) and b) shows the retrieved responses with the position of the reference source at $x = 2500$ m by deconvolution and cross-coherence, respectively. The retrieved responses correspond to an acquisition geometry with both borehole sources and receivers. Next, assuming that the source power spectrum can be estimated, we use cross-correlation SI and divide the power spectrum on both sides of equation (7) and the result is shown in Fig. 4 c). Fig. 4 d) shows the reference response directly modelled with a homogeneous overburden. Fig. 5 shows the counterpart of Fig. 4 but with a reference source position at $x = 3000$ m. The *clamped boundary condition* can be

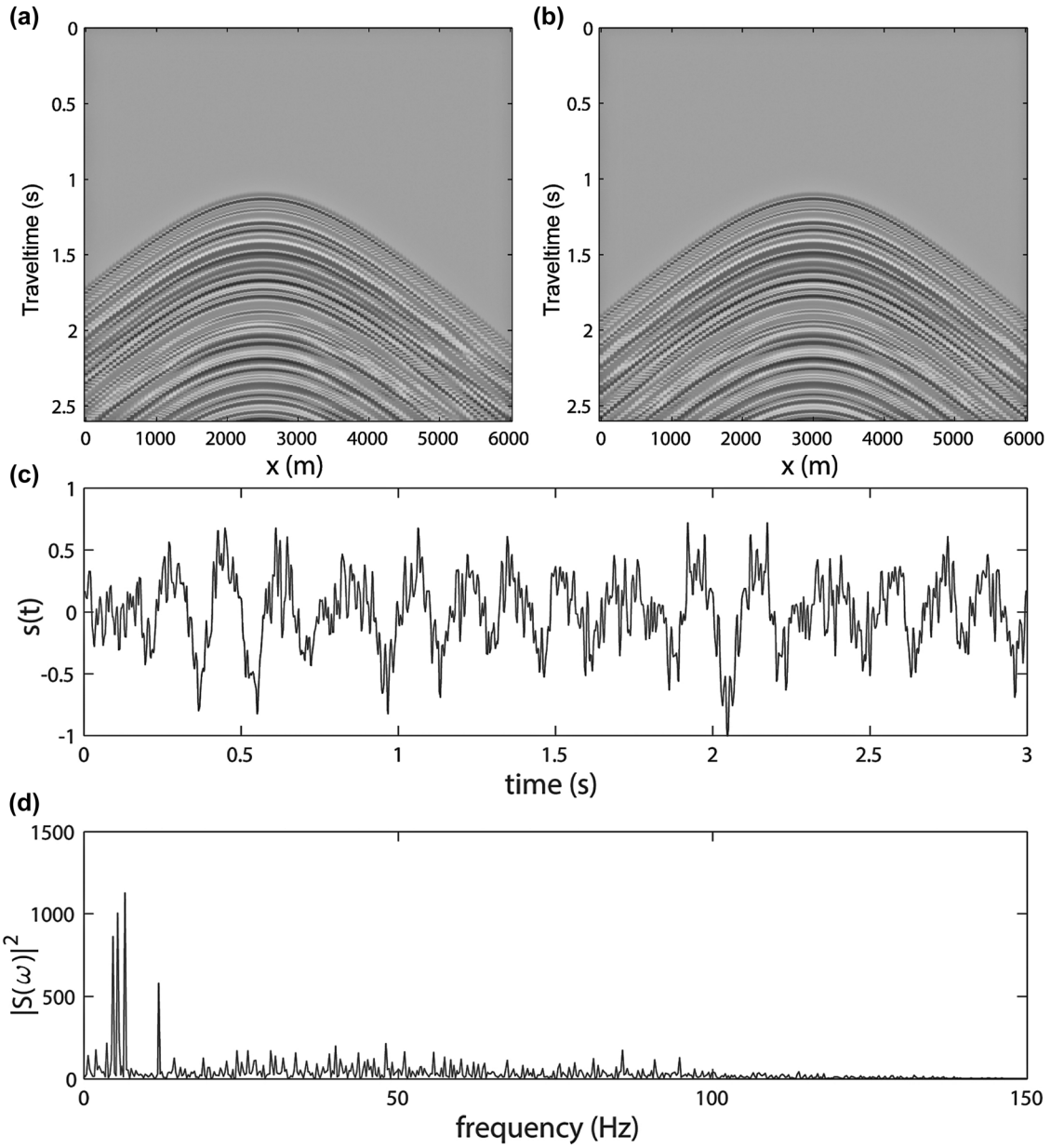

Figure 3 Drill-bit source function and recorded common-source gathers. a) Common-source gather at $x = 2500$ m and b) at $x = 3000$ m. c) Modelled drill-bit source function. d) Power spectrum of the modelled drill-bit function. The drill-bit source function is modelled as a three-cone roller bit with each cone composed of three teeth rows (Poletto *et al.* 2004), the weight on bit of 130 kN, 60-bit revolutions per minute, and a normalized speed amplitude of 0.3 (Aarrestad and Kyllingstad 1988). $s(t)$ and $|S(\omega)|^2$ denote the source time function and its power spectrum, respectively.

observed in both Fig. 4 a) and b) and Fig. 5 a) and b) as the wavefield vanishes at zero offset except at time zero. In addition, as discussed before, the retrieved response by cross-coherence in Fig. 4 b) and Fig. 5 b) also appears more balanced and stable compared with the response by deconvolution in Fig. 4 a) and Fig. 5 a).

Different source signals

In reality, the drill-bit signal varies at different positions; thus, for this example, we modelled 81 different drill-bit signals at each source position indicated in Fig. 2. Fig. 6 a) shows the modelled drill-bit source function $s(t)$ at $x = 3000$ m,

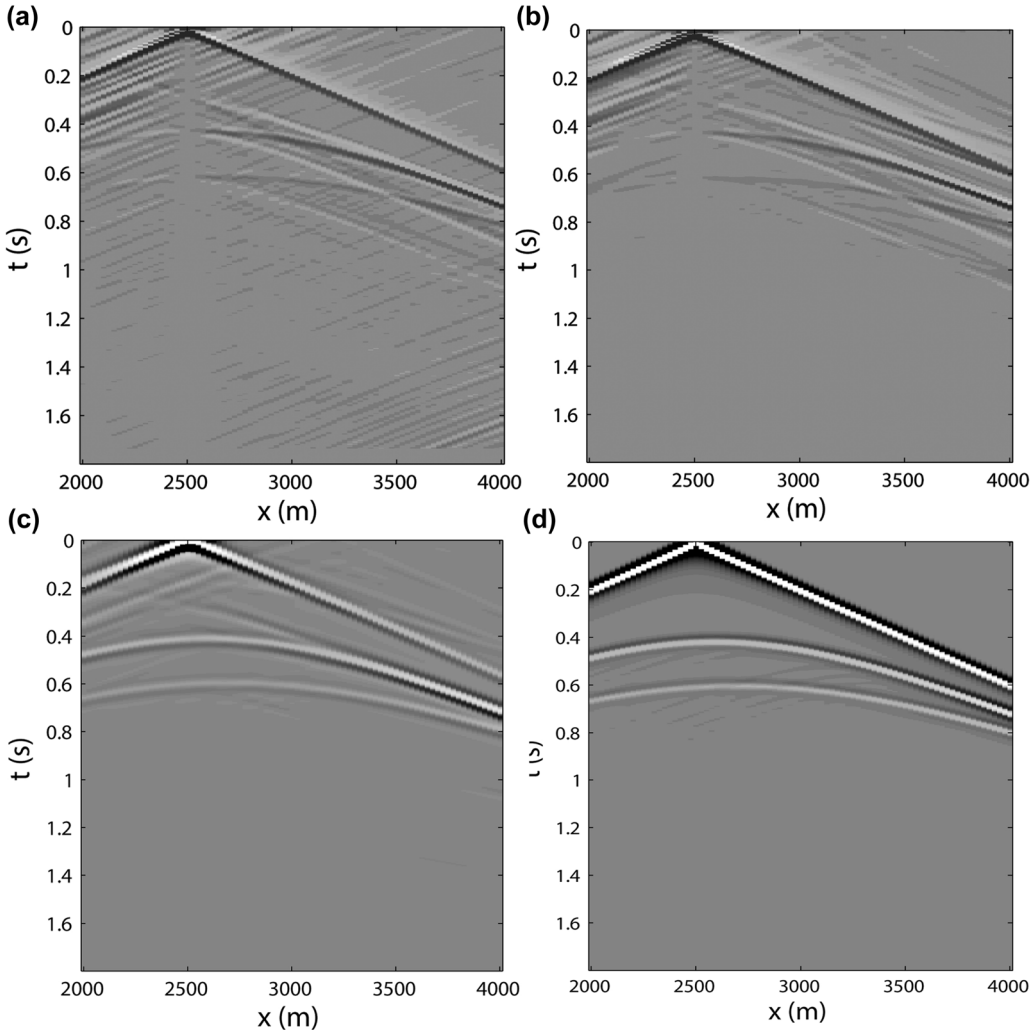

Figure 4 Comparison of the retrieved responses with the reference response. The virtual response of the source at $x = 2500$ m retrieved by a) deconvolution, b) cross-coherence, and c) cross-correlation. d) The reference response modelled with a homogeneous overburden. Both a) and b) do not require any knowledge of the source function $s(t)$, except that $s(t)$ does not change with changing drill-bit positions, whereas c) requires the power spectrum $|S(\omega)|^2$ to be known.

and panel b) shows the pilot signal $\tilde{s}(t)$ with about 5% noise (due to the machinery, electricity, etc.). The noise $\tilde{s}(t) - s(t)$ is shown in panel c). Then we deconvolve the recorded surface drill-bit data using both the exact source signal $s(t)$ and the pilot signal $\tilde{s}(t)$, respectively. Fig. 7 a) shows a raw common-source gather at $x = 3000$ m, and panels b) and c) show the pilot-deconvolved common-source gathers using $s(t)$ and $\tilde{s}(t)$, respectively. The retrieved responses using inter-source cross-correlation interferometry (equation 2) are shown in Fig. 8. Energy normalization is applied after the interferometry process for panels b) and d), which use the noise-contaminated pilot signal $\tilde{s}(t)$. No energy normalization is applied for panels a) and c), which use the exact source signal $s(t)$.

Using the above procedure, we retrieve common-source gathers for a source at each drill-bit position and virtual receivers at all other drill-bit positions. Then we migrate the retrieved responses from the $\tilde{s}(t)$ pilot-deconvolved data using one-way prestack depth migration (Thorbecke, *et al.*, 2004) with a simple homogeneous velocity of 2750 m/s (2500 m/s+10% error). The result is shown in Fig. 9 a). Note that the velocity in the layer where the drill-bit

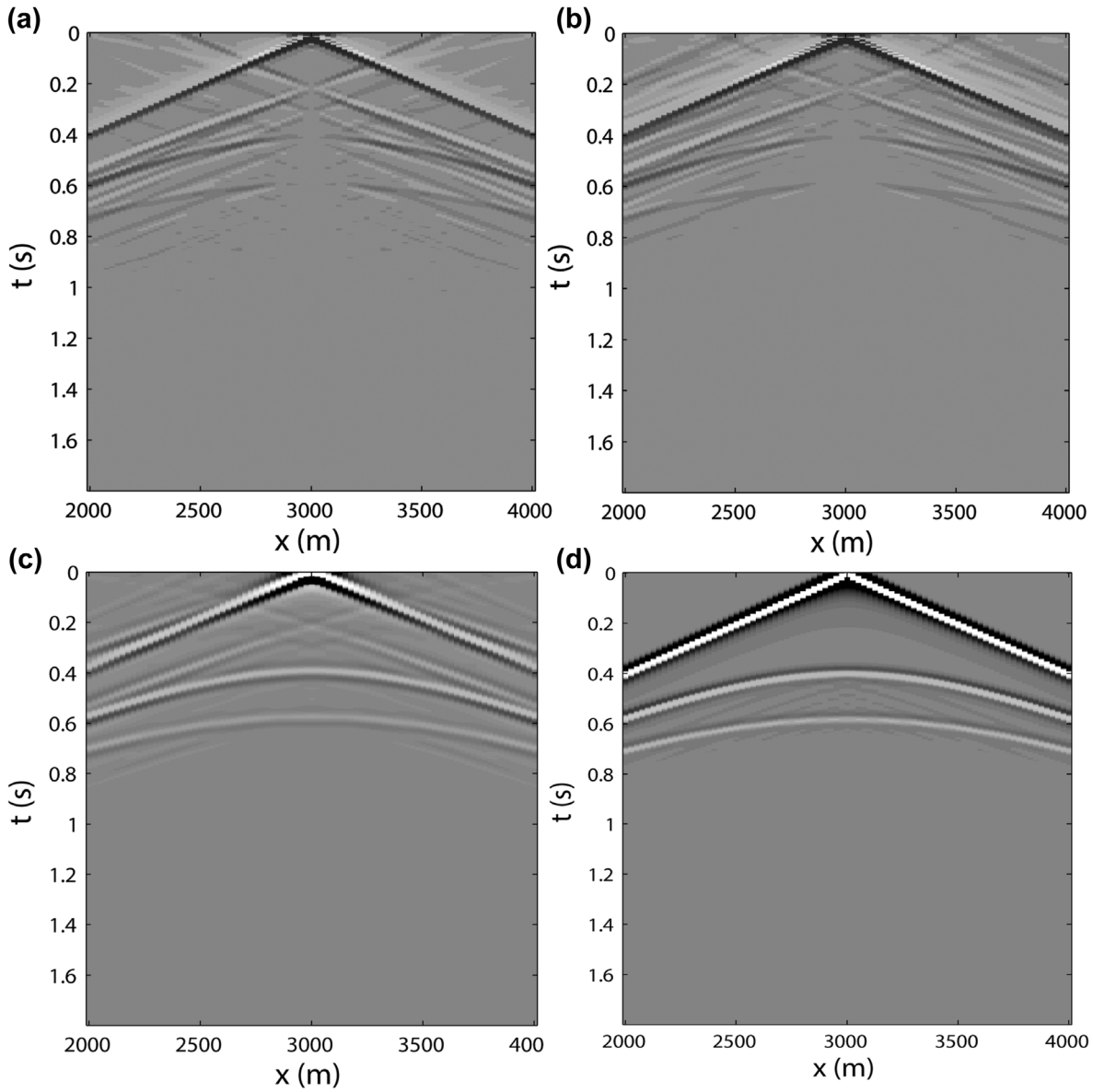

Figure 5 As Fig. 4, but for the source at $x = 3000$ m.

positions are situated is 2500 m/s and the velocities of the layers below it are 3300 m/s and 4000 m/s. Fig. 9 b) shows a conventional image of the subsurface reflectors obtained from the surface seismic reflection data using the 10% erroneous migration velocity. We can see that the deep reflectors are mispositioned more severely in Fig. 9 b) than in Fig. 9 a).

Because we use the total wavefields in the interferometry process and we only have one-sided illumination with a finite number of receivers at the surface, non-physical reflection appears in all retrieved responses. In Fig. 8, non-physical reflections (indicated by the arrows) appear before the first primary reflection. This is due to the cross-correlation of the upgoing direct field with the upgoing internal multiple from the second layer (indicated by the arrow in Fig. 7). In the conventional redatuming to a horizontal well, in which receivers are used, often only the direct arrival is used for correlation (e.g., Bakulin and Calvert (2006)). This eliminates the retrieval of some possible non-physical reflections. Mehta *et al.* (2007) show that using wavefield separation and correlating the direct arrival in the downgoing wavefield with the upgoing arrivals further improve the retrieved results, as some more non-physical reflections are not retrieved. Further, tapering the traces that are

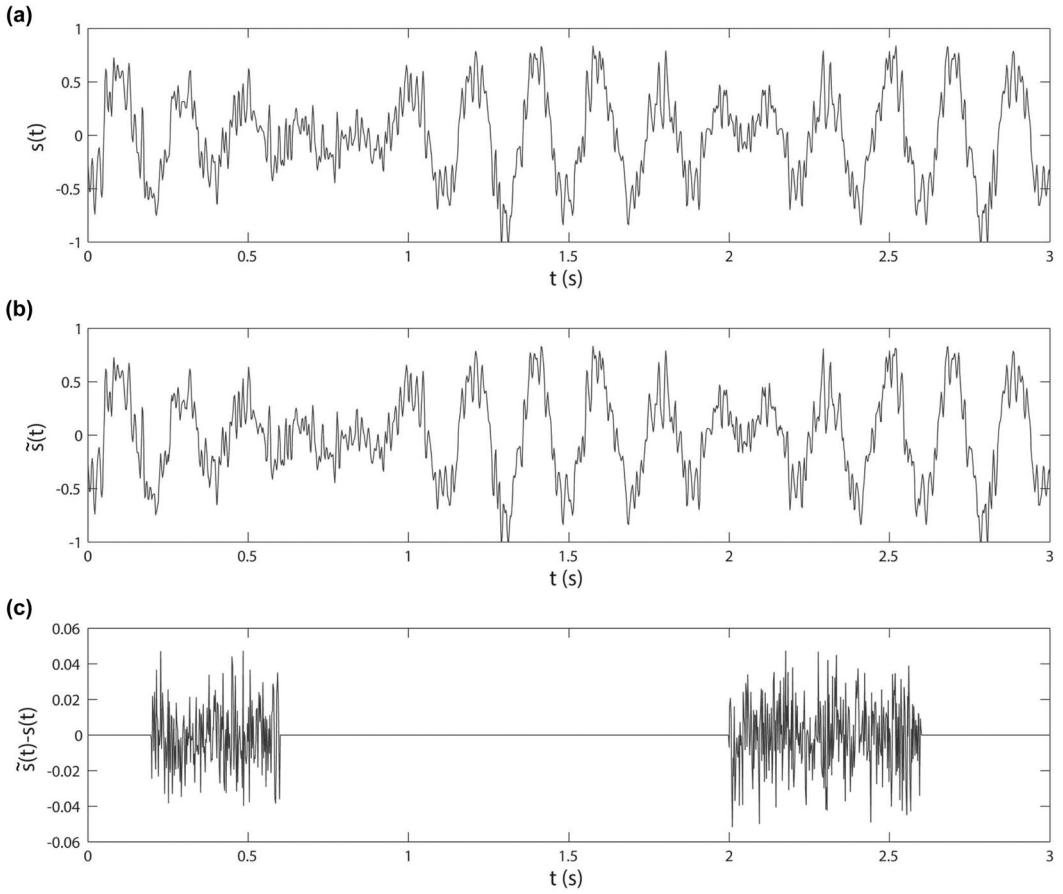

Figure 6 Modelled drill-bit signal. a) The exact drill-bit source function $s(t)$. b) Estimate of the signal $\tilde{s}(t)$. c) The noise added to the estimated signal, which is up to 5% of the drill-bit signal.

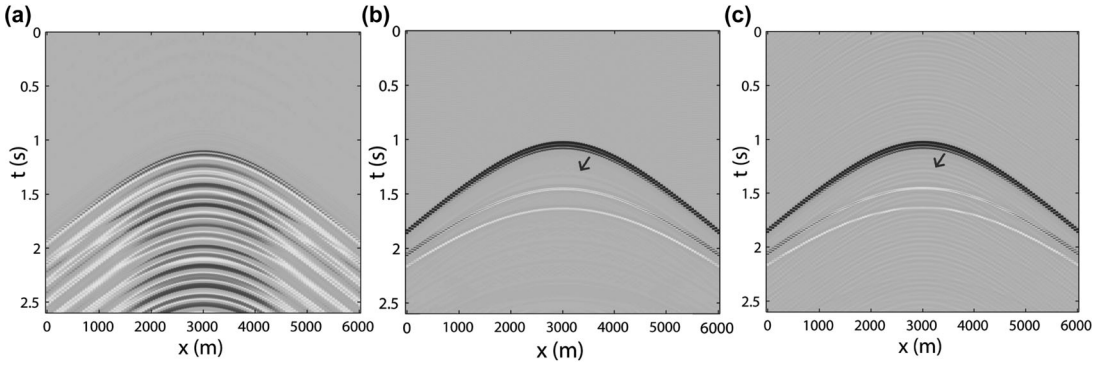

Figure 7 Modelled common-source gather and pilot-deconvolved results. a) Raw common-source gather from drilling noise at $x = 3000$ m. Pilot-deconvolved common-source gathers using b) the exact source signal $s(t)$ and c) the noise-contaminated pilot signal $\tilde{s}(t)$. The arrow indicates the internal multiple from the second layer, which arrives about 0.2 second after the direct waves.

recorded at positions far from the stationary-phase positions would reduce some of the artefacts in the retrieved response, which appear as straight lines extending out from the retrieved first primary reflections in Fig. 8.

DISCUSSION

From the above results, it is clear that the information about the drill-bit noise is essential. In practical applications, the

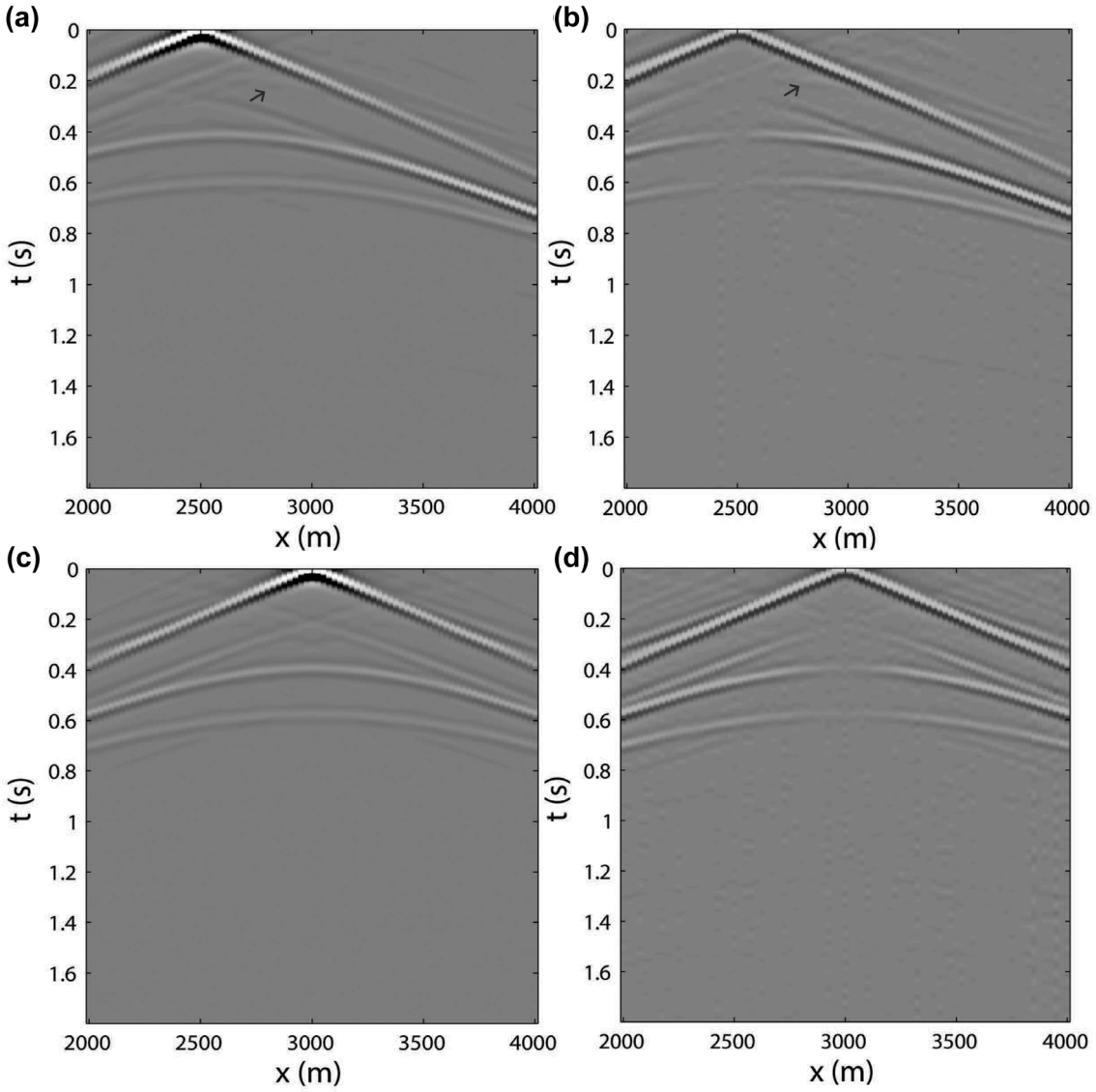

Figure 8 Retrieved common-source response at the drill-bit positions. The top row corresponds to the virtual drill-bit receiver data from a virtual source at $x = 2500$ m and the bottom row from a virtual source at $x = 3000$ m. a) and c) are retrieved after using the exact drill-bit source function $s(t)$ for pilot deconvolution, and b) and d) are retrieved after using $\tilde{s}(t)$ for pilot deconvolution and applying energy normalization to the retrieved response. The arrow indicates the non-physical reflection identified as the cross-correlation of the direct waves and the internal multiples.

useful signal from the pilot at the drill-bit should have sufficient signal-to-noise ratio. When the level of the interfering noise (e.g., from the noise inside the borehole) is too high, the method might not work.

The method we propose will work best with receivers that can be left in the field for the time of the drilling. This means that its natural area of application would be with receiver arrays on land or with ocean-bottom stations or cables. In all three cases, the receiver spacing should not allow aliasing of the recorded wavefields.

Note that the length of the receiver array (extent of the network) would dictate the positions of the drill-bit between which a reflection response can be retrieved. The two drill-bit positions and the receiver geometry must be such that the receivers cover the stationary-phase region for retrieval of reflections between the two drill-bit positions.

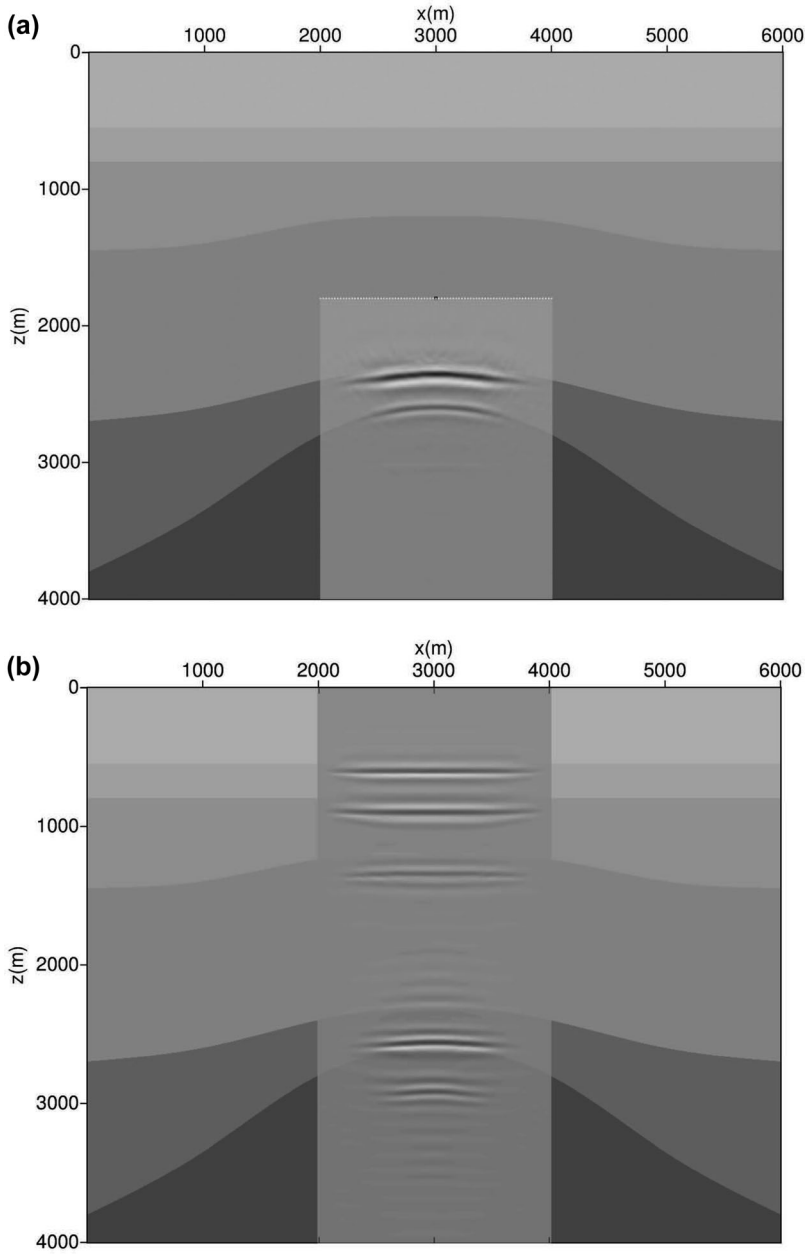

Figure 9 Migration images a) using retrieved virtual reflection responses at the drill-bit positions and b) using conventional surface seismic reflection data. The background indicates the true velocity model. Image a) is obtained using a homogeneous velocity model of 2750 m/s (2500 m/s+10% error), whereas image b) is obtained using the 10% erroneous velocities of the whole model.

CONCLUSION

We have applied inter-source SI to numerically simulated drill-bit signal. Contrary to Green's function retrieval between receivers using mutually uncorrelated non-transient sources with unknown signals, a successful application of inter-source SI requires the non-transient sources to have the same signal. We show that, if this condition is met, deconvolution or cross-coherence interferometry can be used to extract useful phase information of the Green's function between source positions, without knowing the source signal itself. In reality, it can be expected that most non-transient sources with known positions, such as drill-bit noise, emit different signals with changing positions. This creates a major problem for applying inter-source SI to non-transient noise sources without knowing their signal (except for the zero-offset response). However, as pilot signals are usually acquired to recover the impulse response of the drill bit, pilot-deconvolved drill-bit data can be utilized with inter-source cross-correlation interferometry to retrieve

virtual reflection responses at drill-bit positions. The retrieved responses are useful for imaging as they have been interferometrically redatumed to the borehole level, thus independent of the velocity accuracy of the overburden. We recommend that pilot signals be measured downhole near the drill bit to get good results after pilot deconvolution because there is additional noise due to drill-string reflections, rig activities, and signal attenuation.

ACKNOWLEDGEMENTS

The authors would like to thank the Research Council of Norway, ConocoPhillips, Det norske oljeselskap, Statoil, and Wintershall for financing the work through the research centre DrillWell - Drilling and Well Centre for Improved Recovery, a research cooperation between IRIS, NTNU, SINTEF, and UiS; and the ROSE consortium at NTNU. The research of D. Draganov is supported by the Division for Earth and Life Sciences (ALW) with financial aid from the Netherlands Organization for Scientific Research (NWO) with VIDI grant 864.11.009. They also thank Joost van der Neut (TU Delft) and the reviewers for their suggestions that helped improve the manuscript.

REFERENCES

Aarrestad T.V. and Kyllingstad Å. 1988. An experimental and theoretical study of a coupling mechanism between longitudinal and torsional drillstring vibrations at the bit. *SPE Drilling Engineering* **3**, 12–18.

Bakulin A. and Calvert R. 2006. The virtual source method: theory and case study. *Geophysics* **71**, SI139–SI150.

Campillo M. and Paul A. 2003. Long-range correlations in the diffuse seismic coda. *Science* **299**, 547–549.

Curtis A., Nicolson H., Halliday D., Trampert J. and Baptie, B. 2009. Virtual seismometers in the subsurface of the Earth from seismic interferometry. *Nature Geoscience* **2**, 700–704.

Draganov D., Wapenaar K., Mulder W., Singer J. and Verdel A. 2007. Retrieval of reflections from seismic background-noise measurements. *Geophysical Research Letters* **34**, L04305.

Draganov D., Campman X., Thorbecke J., Verdel A. and Wapenaar K. 2009. Reflection images from ambient seismic noise. *Geophysics* **74**, A63–A67.

Draganov D., Campman X., Thorbecke J., Verdel A. and Wapenaar K. 2013. Seismic exploration-scale velocities and structure from ambient seismic noise (>1 Hz). *Journal of Geophysical Research: Solid Earth* **118**, 4345–4360.

Eidsvik J. and Hokstad K. 2006. Positioning drill-bit and look-ahead events using seismic traveltime data. *Geophysics* **71**, F79–F90.

Gerstoft P., Sabra K., Roux P., Kuperman W. and Fehler M. 2006. Green's functions extraction and surface-wave tomography from microseisms in Southern California. *Geophysics* **71**, SI23–SI31.

Haldorsen J.B., Miller D.E. and Walsh J.J. 1995. Walk-away VSP using drill noise as a source. *Geophysics* **60**, 978–997.

Lobkis O.I. and Weaver R.L. 2001. On the emergence of the Green's function in the correlations of a diffuse field. *The Journal of the Acoustical Society of America* **110**, 3011–3017.

Malusa M., Poletto F. and Miranda F. 2002. Prediction ahead of the bit by using drill-bit pilot signals and reverse vertical seismic profiling (RVSP). *Geophysics* **67**, 1169–1176.

Mehta K., Sheiman J., Snieder R. and Calvert R. 2007. The virtual source method applied to Mars field OBC data for time-lapse monitoring. *SEG Expanded abstracts*, 2914–2918.

Miller D., Haldorsen J. and Kostov C. 1990. Methods for deconvolution of unknown source signatures from unknown waveform data. *U.S. Patent* **4922362**.

Nakata N., Snieder R., Tsuji T., Larner K. and Matsuoka T. 2011. Shear wave imaging from traffic noise using seismic interferometry by cross-coherence. *Geophysics* **76**, SA97–SA106.

Panea I., Draganov D., Vidal C.A. and Mocanu V. 2014. Retrieval of reflections from ambient noise recorded in Mizil area, Romania. *Geophysics* **79**, Q31–Q42.

Poletto F., Corubolo P. and Comelli P. 2010. Drill-bit seismic interferometry with and without pilot signals. *Geophysical Prospecting* **58**, 257–265.

Poletto F., Malusa M., Miranda F. and Tinivella U. 2004. Seismic while drilling by using dual sensors in drill strings. *Geophysics* **69**, 1261–1271.

Poletto F. and Miranda F. 2004. *Seismic While Drilling: Fundamentals of Drill-Bit Seismic for Exploration*. Pergamon. 35.

Poletto F., Miranda F., Corubolo P., Schleifer A. and Comelli P. 2014. Drill-bit seismic monitoring while drilling by downhole wired-pipe telemetry. *Geophysical Prospecting* **62**, 702–718.

Poletto F., Rocca F. and Bertelli L. 2000. Drill-bit signal separation for RVSP using statistical independence. *Geophysics* **65**, 1654–1659.

Rector J. and Hardage B. 1992. Radiation pattern and seismic waves generated by a working roller-cone drill bit. *Geophysics* **57**, 1319–1333.

Rector J. and Marion B. 1991. The use of drill-bit energy as a downhole seismic source. *Geophysics* **56**, 628–634.

Roux P., Sabra K.G., Gerstoft P., Kuperman W.A. and Fehler M.C. 2005. P-waves from cross-correlation of seismic noise. *Geophysical Research Letters* **32**, L19303.

Ruigrok E., Campman X. and Wapenaar K. 2011. Extraction of P-wave reflections from microseisms. *Comptes Rendus Geoscience* **343**, 512–525.

Sabra K.G., Gerstoft P., Roux P., Kuperman W.A. and Fehler M.C. 2005a. Extracting time-domain Green's function estimates from ambient seismic noise. *Geophysical Research Letters* **32**, L03310.

Sabra K.G., Gerstoft P., Roux P., Kuperman W.A. and Fehler M.C. 2005b. Surface wave tomography from microseisms in Southern California. *Geophysical Research Letters* **32**, L14311.

Shapiro N.M. and Campillo M. 2004. Emergence of broadband Rayleigh waves from correlations of the ambient seismic noise. *Geophysical Research Letters* **31**, L07614.

Shapiro N.M., Campillo M., Stehly L. and Ritzwoller M.H. 2005. High-resolution surface-wave tomography from ambient seismic noise. *Science* **307**, 1615–1618.

Snieder R. 2004. Extracting the Green's function from the correlation of coda waves: a derivation based on stationary phase. *Physical Review E* **69**(4), 046610.

Snieder R., Wapenaar K., and Larner K. 2006. Spurious multiples in seismic interferometry of primaries. *Geophysics* **71**, SI111–SI124.

Thorbecke J. and Draganov D. 2011. Finite-difference modeling experiments for seismic interferometry. *Geophysics* **76**, H1–H18.

Thorbecke J., Wapenaar K. and Swinnen G. 2004. Design of one-way wavefield extrapolation operators, using smooth functions in WLSQ optimization. *Geophysics* **69**, 1037–1045.

Tonegawa T. and Nishida K. 2010. Inter-source body wave propagations derived from seismic interferometry. *Geophysical Journal International* **183**, 861–868.

Vasconcelos I. and Snieder R. 2008a. Interferometry by deconvolution: Part 1 - Theory for acoustic waves and numerical examples. *Geophysics* **73**, S115–S128.

Vasconcelos I. and Snieder R. 2008b. Interferometry by deconvolution: Part 2 - Theory for elastic waves and application to drill-bit seismic imaging. *Geophysics* **73**, S129–S141.

Wapenaar K. 2004. Retrieving the elastodynamic Green's function of an arbitrary inhomogeneous medium by cross correlation. *Physical Review Letters* **93**, 254301.

Wapenaar K. and Fokkema J. 2006. Greens function representations for seismic interferometry. *Geophysics* **71**, SI33–SI46.

Xu Z., Juhlin C., Gudmundsson O., Zhang F., Yang C., Kashubin A. *et al.* 2012. Reconstruction of subsurface structure from ambient seismic noise: an example from Ketzin, Germany. *Geophysical Journal International* **189**, 1085–1102.

Yang Y., Ritzwoller M.H., Levshin A.L. and Shapiro N.M. 2007. Ambient noise Rayleigh wave tomography across Europe. *Geophysical Journal International* **168**, 259–274.

Zhan Z., Ni S., Helmberger D.V. and Clayton R.W. 2010. Retrieval of Moho-reflected shear wave arrivals from ambient seismic noise. *Geophysical Journal International* **182**, 408–420.